Chin. J. Mech. Eng. (2017) 30:352–362
DOI 10.1007/s10033-017-0085-5

ORIGINAL ARTICLE

Thermodynamic Behavior Research Analysis of Twin-roll Casting Lead Alloy Strip Process

Chengcan JIANG[1] · **Yannian RUI**[1]

Received: 17 November 2016 / Revised: 30 December 2016 / Accepted: 5 January 2017 / Published online: 17 March 2017

Abstract The thermodynamic behavior of twin-roll casting (TRC) lead alloy strip process directly affects the forming of the lead strip, the quality of the lead strip and the production efficiency. However, there is little research on the thermodynamics of lead alloy strip at home and abroad. The TRC lead process is studied in four parameters: the pouring temperature of molten lead, the depth of molten pool, the roll casting speed, and the rolling thickness of continuous casting. Firstly, the thermodynamic model for TRC lead process is built. Secondly, the thermodynamic behavior of the TRC process is simulated with the use of Fluent. Through the thermodynamics research and analysis, the process parameters of cast rolling lead strip can be obtained: the pouring temperature of molten lead: 360–400 °C, the depth of molten pool: 250–300 mm, the roll casting speed: 2.5–3 m/min, the rolling thickness: 8–9 mm. Based on the above process parameters, the optimal parameters(the pouring temperature of molten lead: 375–390 °C, the depth of molten pool: 285–300 mm, the roll casting speed: 2.75–3 m/min, the rolling thickness: 8.5–9 mm) can be gained with the use of the orthogonal experiment. Finally, the engineering test of TRC lead alloy strip is carried out and the test proves the thermodynamic model is scientific, necessary and correct. In this paper, a detailed study on the thermodynamic behavior of lead alloy strip is carried out and the process parameters of lead strip forming are obtained through the research, which provide an effective theoretical guide for TRC lead alloy strip process.

Keywords TRC lead alloy strip · Thermodynamic model · Thermodynamic behavior · Theoretical guide

1 Introduction

Lead alloy strips are widely used in electrolytic copper and zinc industry. Their electrochemical properties and mechanical properties have a direct impact on the energy consumption of the electric product and the service life of anode [1–3]. In order to reduce the energy consumption and improve the life of the anode, limitation pretreatments, shot peening, sand blasting, KF solution electrolysis and plating methods have been used [4, 5]. But these methods have increased the additional energy consumption. PRENGAMAN, et al. [6–8], thought rolling could improve the mechanical properties of lead alloy to reduce its microstructure defects and improve the service life at the same time. PETROVA, et al. [9–11], had a series of rolling experiments for Pb-Ag-Ca and Pb-Ag-Co alloys. They thought it could improve the corrosion resistance of alloy and reduce the oxygen evolution potential. After that it could enhance the electrochemical properties of alloy. HILGER [12] pointed out that rolling could accelerate the aging of Pb-Ca-Sn alloy and increase the mechanical properties. Meanwhile ALBERT, et al. [13], considered the

Supported by National Hi-tech Research and Development Program of China (863 Program, Grant No. 2012AA063506), Natural Science Foundation of Jiangsu Higher Education Institutions of China (Grant No. 14KJB460026), and Suzhou Science and Technology Support Program of China (Grant No. SS201344).

✉ Chengcan JIANG
jiang198854@163.com

[1] School of Mechanical and Electric Engineering, Soochow University, Jiangsu 215021, China

rolling could improve the quaternary alloy's mechanical properties of Pb–Ca-Sn-Al alloy. Similar researches were also done by FU, et al. [14], WILSON, et al. [15], RASP, et al. [16], JESWIET [17] and TSAO, et al. [18–20].

The traditional lead alloy strip is usually prepared by multi-pass rolling process, and this method has many disadvantages such as large labor intensity, high rate of geometry scrap, low rate of finished product and so on. To improve the method of forming lead alloy strip, TRC process will be studied in this paper.

TRC lead can increase the capacity of the production of lead strips in a cost-efficient way. Therefore, the TRC process becomes important and offers a great potential for industrial application. Compared to the conventional thin sheet production, TRC is more economic and energy-efficient due to the saving of process steps [21].

The working principle of TRC lead is shown in Fig. 1, it combines the continuous casting and hot rolling together and enables the production of strips with improved microstructure properties. In contrast to copper and aluminum, which are manufactured successfully by TRC, TRC lead alloy is currently at the development stage. Since 1980s, research groups throughout the world(USA, Germany, Japan and Italy) have been dealing with the development of the technology and the characterization of the materials in the TRC lead alloy state [22].

The paper mainly revolves around the quality of continuous casting lead in the TRC process. The four parameters which affect the quality of lead alloy: the pouring temperature of molten lead, the depth of molten pool, the roll casting speed and the rolling thickness of continuous castings are studied. The optimized process parameters can be worked out with the use of FLUENT. Based on these, the actual optimum process parameters can be gained which shows a better conductivity and higher mechanical performance compared to the multi-pass rolling process.

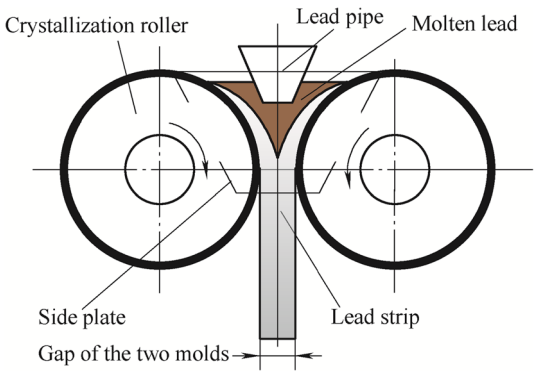

Fig. 1 Working principle of TRC lead

2 Thermodynamic Model

2.1 Heat Transfer Model

Researches show that the continuous casting process of lead is that molten lead is pulled at a certain speed from the gap of the two molds. In the process, heat transfer from the center of slab to the surface of shell which depends on the thermal physical properties of lead alloy and boundary conditions of slab.

Assuming that the thickness direction of lead tape is the x axis, width direction is the y axis and casting direction is the z axis. The temperature distribution of lead strip's cross-section is $T(x, y, z)$. Considering the symmetry of lead zone and its cooling, it can take 1/4 of the zone as the research object. The coordinate system is built and shown in Fig. 2.

The process of TRC lead makes the following assumptions:

(1) The process of TRC lead is taken the same continuum (including solid zone, liquid phase zone and solid–liquid mushy zone),
(2) The density of each phase is a constant,
(3) The change of the specific heat c is shown by the transformation enthalpy method in the process,
(4) The calculation does not consider the influence of the latent heat of phase change.

Infinitesimal body will be downward movement with the same speed of the coordinate system which is fixed on the slab. The transient thermal equilibrium process of any infinitesimal body in cartesian coordinate system is shown in Fig. 3.

According to the fourier heat conduction law, the three-dimensional differential equation of heat transfer for slab solidification process is [23–25]:

$$0 = \rho c\frac{\partial T}{\partial t} - \rho v c\frac{\partial T}{\partial z} - \frac{\partial}{\partial x}\left(\lambda\frac{\partial T}{\partial x}\right) - \frac{\partial}{\partial y}\left(\lambda\frac{\partial T}{\partial y}\right). \quad (1)$$

According to the Kirchhoff Transformation, there are two equations in the model [26]:

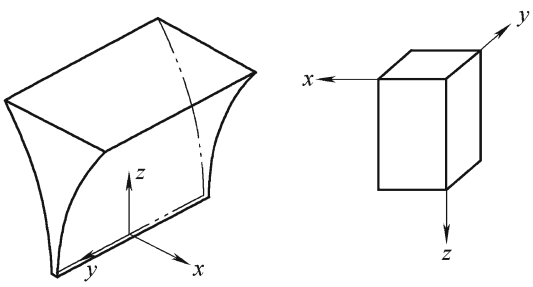

Fig. 2 Figure of coordinate selection

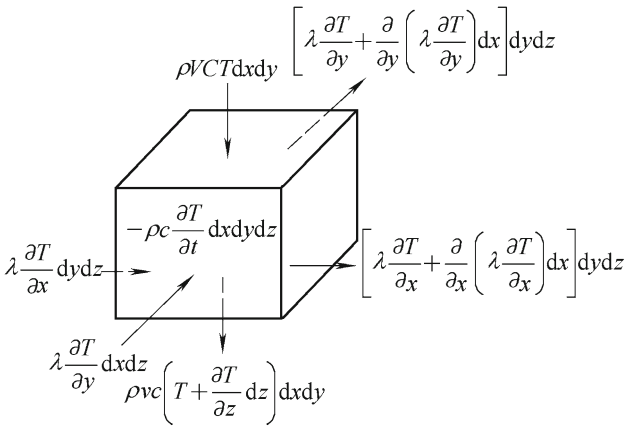

Fig. 3 Sketch map of the space element

$$\Phi=\int_{T_0}^{T}\frac{\lambda(T)}{\lambda_0}\mathrm{d}T, \tag{2}$$

$$H=\int_{T_0}^{T}c(T)\mathrm{d}T, \tag{3}$$

where Φ—Transformation temperature,
H—Transition enthalpy,
$\lambda(T)$, $c(T)$—Thermal coefficient and specific heat of infinitesimal body when the temperature is T,
λ_0—Heat conductivity of infinitesimal body when the temperature is 0 °C.

When putting Eqs. (2) and (3) into Eq. (1), then Eq. (1) will become Eq. (4) for heat transfer modeling of the casting solidification process of the lead strip [27]:

$$\rho\frac{\partial H}{\partial t}=\rho v\frac{\partial H}{\partial z}+\lambda_0\left(\frac{\partial^2\Phi}{\partial x^2}+\frac{\partial^2\Phi}{\partial y^2}\right). \tag{4}$$

2.2 Mechanical Model

The process of TRC lead is fairly complex. It includes heat transfer, solidification phase transformation and plastic deformation. So the rigid-viscoplastic FEM is used to solve it in this research [28–30].

According to the variation principle of Markov, the mechanical model is expressed by Eq. (5):

$$\phi_0=\int_V E\left(\overset{0}{\varepsilon}_{ij}\right)\mathrm{d}V-\int_{S_F}F_i v_i\mathrm{d}S,$$

$$E\left(\overset{0}{\varepsilon}_{ij}\right)=\int_0^{\overset{0}{\varepsilon}}\sigma\mathrm{d}\overset{0}{\varepsilon}, \tag{5}$$

where $E\left(\overset{0}{\varepsilon}_{ij}\right)$—Work function, eV,
V—Volume deformation, m^3,
S—Surface deformation, m^2,
σ—Equivalent stress, MPa,
$\overset{0}{\varepsilon}$—Equivalent strain rate, 1/s,
F_i—Specified force on the boundary, N,
v_i—Velocity field in deformation body, m/s.

2.3 Initial Conditions and Boundary Conditions

2.3.1 Initial Conditions

For Eqs. (4) and (5), the initial conditions are

$$\begin{cases}T=T_0\ (x\geq 0,y\geq 0,z\geq 0,t\geq 0),\\ T(x,0,0)|_{x=0}=T_b\ (t=0),\\ x_s|_{t=0}=0,\end{cases} \tag{6}$$

where T_0—Pouring temperature, °C,
T_b—Surface temperature of early casting, °C,
x_s—Thickness of casting solidification, m.

2.3.2 Boundary Condition

Heat from the molten lead to crystallization roller is taken away by the high-speed flow of cooling water in the TRC process. After that it will form a certain thickness of the strip. Based on principles of lead strip without leak and defect, the average heat flux density of crystal roller's cooling can be calculated according to heat balance relationship:

$$\overline{q}=\frac{Q_{\mathrm{W}}c_{\mathrm{W}}\Delta T_{\mathrm{W}}}{F}, \tag{7}$$

where $\overline{q}$—Average heat flux density, $\mathrm{W/m^2}$,
Q_{W}—Cooling water flow rate, $\mathrm{m^3/s}$,
c_{W}—Specific heat of water, kJ/(kg °C),
ΔT_{W}—Difference of the water temperature in and out of crystallizer, °C,
F—Effective heating area of crystallizer, $\mathrm{m^2}$.

3 Finite Element Simulation

3.1 Geometric Model

The area of TRC lead is made up of two relative rotations of forming rollers and sealing plates. It is shown in Fig. 4.

3.2 Definition of Material Parameters

The experimental material is lead alloy of Pb-Ag-Ca. Its chemical compositions(mass fraction) are listed as follows:
$\omega(\mathrm{Ag})=1.5\%$–$2.0\%$
$\omega(\mathrm{Ca})=0.08\%$, $\omega(\mathrm{Sn})=0.006\%$,
$\omega(\mathrm{Sb})\leq 0.02\%$, $\omega(\mathrm{Cu})\leq 0.06\%$,
$\omega(\mathrm{Fe})\leq 0.012\%$, $\omega(\mathrm{Bi})\leq 0.03\%$,

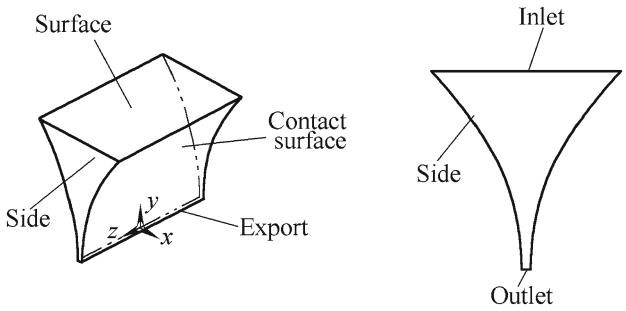

Fig. 4 Model of continuous casting area

$\omega(\mathrm{As}) \leq 0.02\%$, the rest are Pb.

In this paper, the thermal physical properties of the material are a function of temperature and they are expressed as follows in the simulation model [31–34].

Density:

$$\rho = 11113.6 - 1.34 \cdot T\left(\mathrm{kg/m^3}\right).$$

Specific heat capacity:

$$C_\mathrm{p} = 246.8 \times T^{-0.08}(\mathrm{J/(kg \cdot K)}).$$

Viscosity:

$$\eta = 4.94 \times 10^{-4} \times e^{\left(\frac{757.1}{T}\right)}(\mathrm{Pa \cdot s}).$$

Heat conductivity:

$$\lambda = 4.21 + 1.2 \times 10^{-2} \cdot T(\mathrm{W/(m \cdot K)}),$$

where T—Temperature, K.

3.3 Mesh Generation

The dimensions of the geometric model are shown in Fig. 5.

For the above model, the free meshing method and the tetrahedral element were used to mesh automatically. Mesh of geometric model is shown in Fig. 6, there are 44438 mesh faces [35].

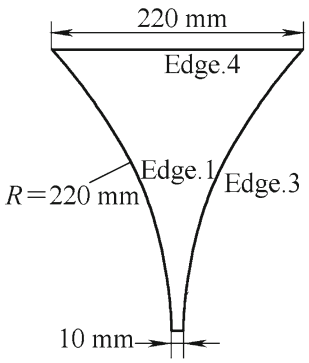

Fig. 5 Dmensions of the geometric model

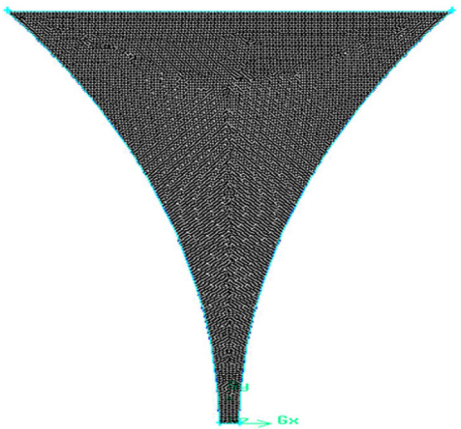

Fig. 6 Results of mesh generation

3.4 Simulation Conditions

This paper mainly researches the pouring temperature of molten lead, the depth of molten pool, the roll casting speed and the rolling thickness which affect the casting area. The simulation values are shown in Table 1.

3.5 Analysis of the Simulation

3.5.1 Effect of Pouring Temperature

The initial conditions for simulation: the depth of molten pool is 300 mm, the roll casting speed is 3 m/min, the rolling thickness is 9 mm, and the pouring temperatures are 360 °C, 400 °C and 440 °C.

It can be seen from Fig. 7 that with the increase of the pouring temperature, the high temperature in the molten pool is gradually close to the outlet. But when the pouring temperature is too low, that will cause high position of solidification. After that the rolling force will become large which is adverse to the process of TRC.

The variation of rolling pressures at different pouring temperature is shown in Fig. 8. From this, it can be seen that under the same conditions, with the increase of the pouring temperature, the same cross-section of the rolling pressure reduces. Meanwhile, the rolling pressure peaks are reduced accordingly and move to the outlet of the casting area.

Table 1 Simulation parameters of continuous casting of TRC lead

Simulation parameters	Parameter values
Pouring temperature T/ °C	360, 400, 440
Depth of molten pool h_m/mm	250, 300, 350
Roll casting speed v_R/(m·min^{-1})	2.5, 3, 3.5
Rolling thickness h_R/mm	8, 9, 10

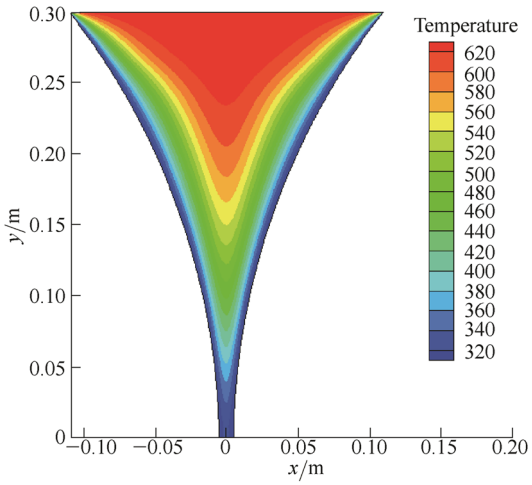

(a) 360°C

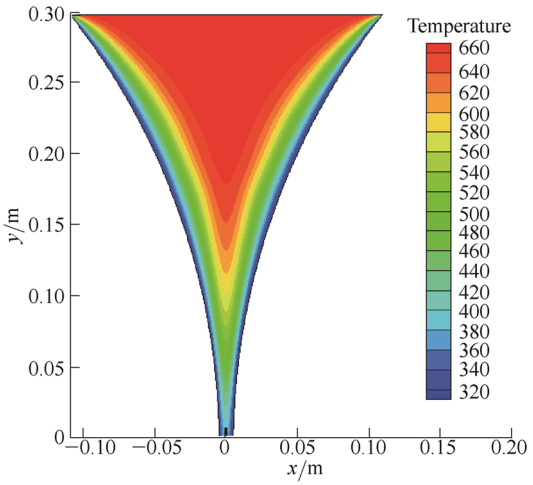

(b) 400°C

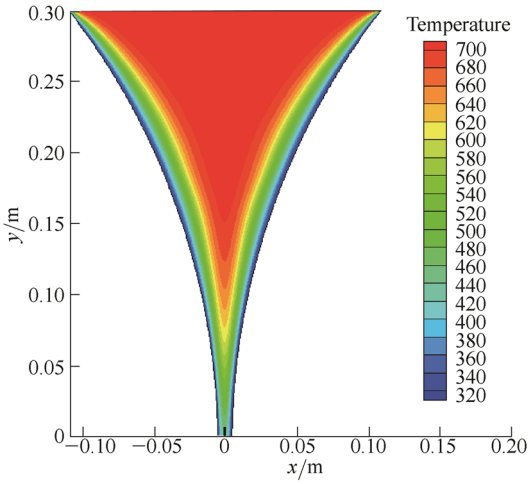

(c) 440°C

Fig. 7 Temperature contour map of casting under different pouring temperatures

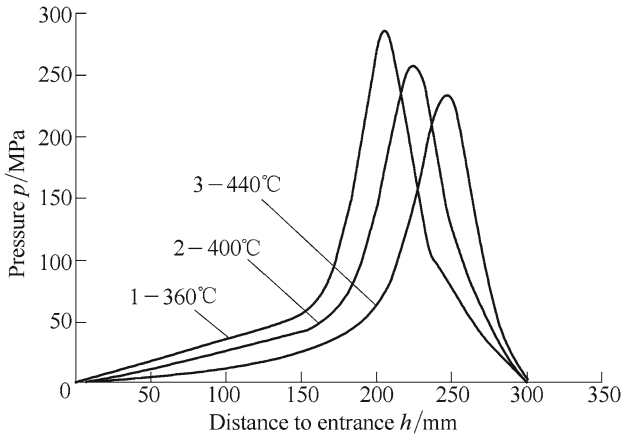

Fig. 8 Influence of pouring temperature on the rolling pressure

3.5.2 Effect of Depth of Molten Pool

The initial conditions for simulation: the pouring temperature is 400 °C, the roll casting speed is 3 m/min, the rolling thickness is 9 mm, and the depths of molten pools are 250, 300 and 350 mm.

It can be seen from Fig. 9 that with the increase of the depth of molten pool, the high temperature in the molten pool is gradually close to the outlet. But when it is too low that will cause local temperature to drop fast. After that the casting of lead strip cannot continue.

The variation of rolling pressures at different depth of molten pool is shown in Fig. 10. From this, it can be seen that under the same conditions, with the reducing of the depth of molten pool, the rolling pressure at the same cross-section decreases.

3.5.3 Effect of Roll Casting Speed

The initial conditions for simulation: the pouring temperature is 400 °C, the depth of molten pool is 300 mm, the rolling thickness is 9 mm, and the roll casting speeds are 2.5 m/min, 3 m/min and 3.5 m/min.

It can be seen from Fig. 11 that with the increase of the roll casting speed, the high temperature in the molten pool is gradually close to the outlet, the solidification time of lead strip is shortened and the thickness of it is also reduced.

The variation of rolling pressures at different roll casting speed is shown in Fig. 12. From Fig. 12, it can be seen that rolling pressure is unimodal. Under the same conditions, with the increase of roll casting speed, the pressure peaks are reduced and the rolling pressure at the same cross-section is decreased.

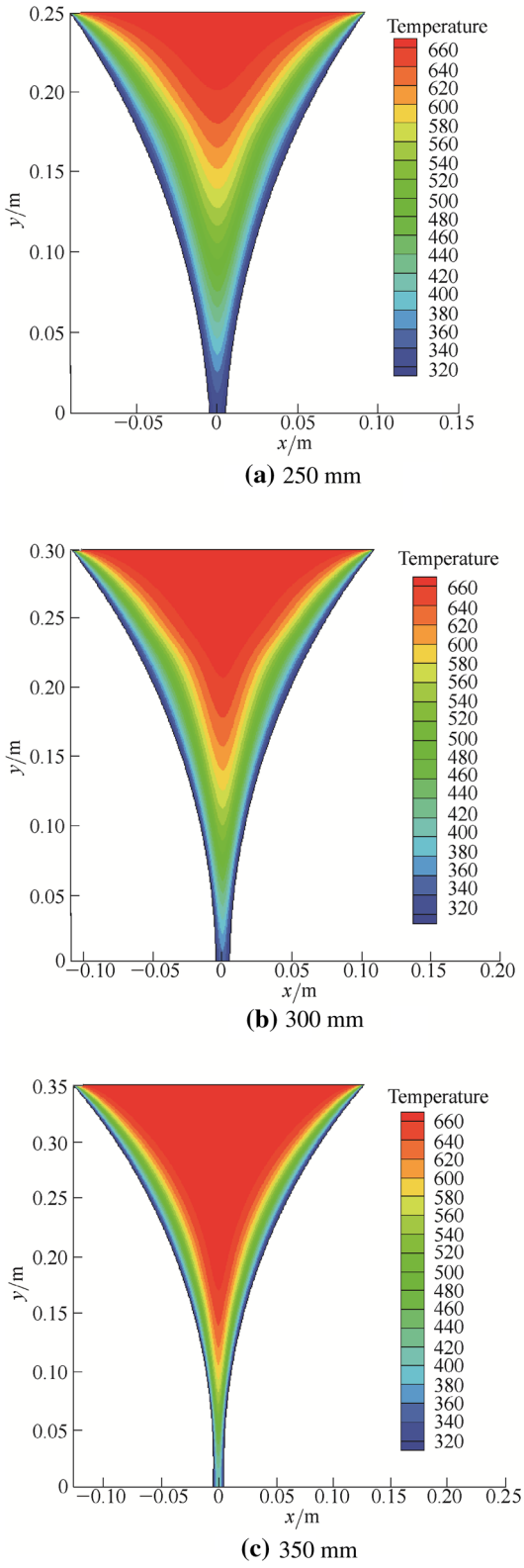

Fig. 9 Temperature contour map of casting under different depth of molten pools

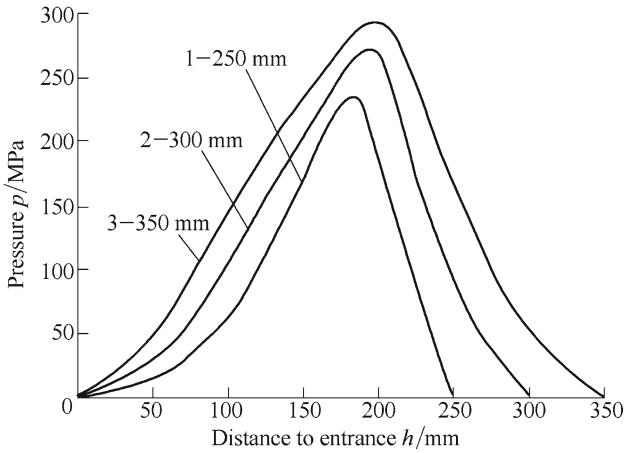

Fig. 10 Influence of depth of molten pool on the rolling pressure

3.5.4 Effect of Rolling Thickness

The initial conditions for simulation: the pouring temperature is 400 °C, the depth of molten pool is 300 mm, the roll casting speed is 3 m/min, and the rolling thicknesses are 8, 9 and 10 mm.

It can be seen from Fig. 13 that with the increase of the rolling thickness, the high temperature in the molten pool is gradually close to the outlet. It will make the strip solidification incomplete, which will lead to low strength of the strip and the broken strip finally.

The variation of rolling pressures at different rolling thickness is shown in Fig. 14. From this, it can be seen that under the same conditions, the rolling pressure peaks are reduced with the increase of the casting roll seam and also has a tendency to move to outlet.

By thermodynamic analysis of four different process parameters of the TRC process, it can initially draw reasonable parameters:

(1) The range of pouring temperature: 360–400 °C,
(2) The range of depth of molten pool: 250–300 mm,
(3) The range of roll casting speed: 2.5–3 m/min,
(4) The range of rolling thickness: 8–9 mm.

4 Experiment Research

Based on the finite element simulation analysis, it has an experiment study of the engineering prototype. The experimental prototype is shown in Fig. 15. In the experiment, the pouring temperature of molten lead is measured by the thermocouple and the depth of molten pool is measured by the ultrasonic liquid level sensor.

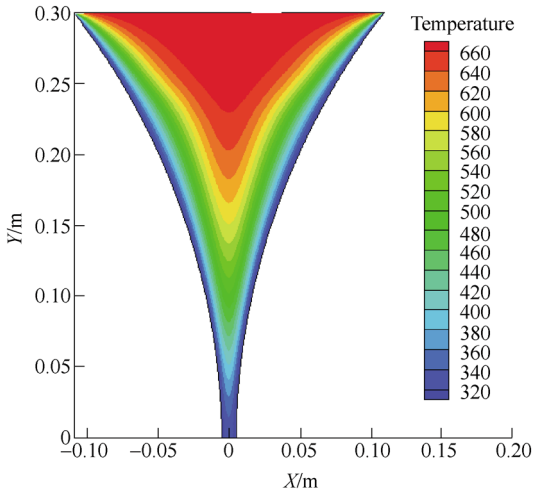

(a) 2.5 m/min

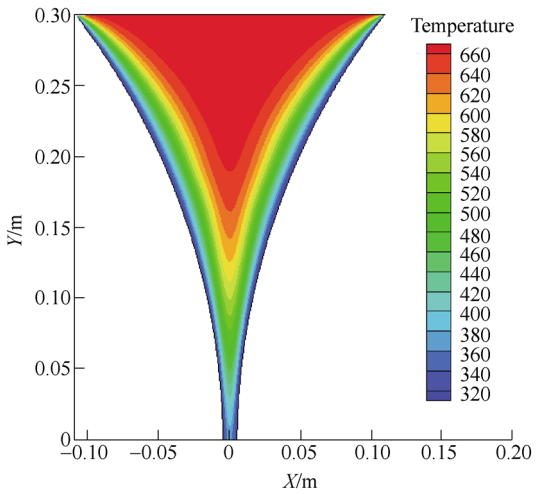

(b) 3 m/min

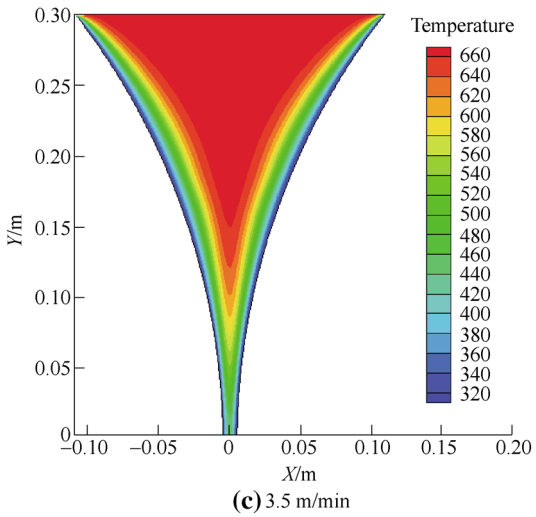

(c) 3.5 m/min

Fig. 11 Temperature contour map of casting under different roll casting speeds

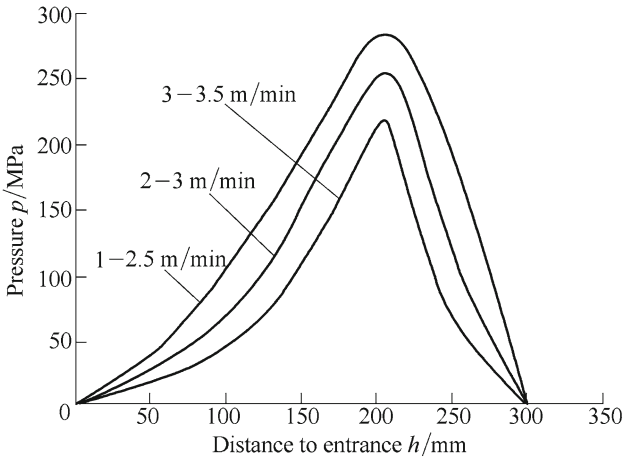

Fig. 12 Influence of roll casting speed on the rolling pressure

The experiment still revolves around the four process parameters which make a difference in the TRC area: the pouring temperature of molten lead, the depth of molten pool, the roll casting speed and the rolling thickness. The experiment is designed with 4 factors and 3 levels with the use of orthogonal method. The distribution of process parameters of TRC lead is shown in Table 2.

Each set of the experiments was repeated 10 times. The electrical conductivity and mechanical properties are used as the assessment indicators of the passing rate. The poor value R of each column in the orthogonal table was calculated by the range analysis. After that the primary and secondary relation of all the factors and the optimal solution can be determined.

With the experiments, the primary and secondary factors that affect TRC process are derived. The pouring temperature of molten lead, the roll casting speed, the depth of molten pool, the rolling thickness and the optimum levels of every factor are as follows:

(1) Pouring temperature of molten lead: 375–390 °C,
(2) Roll casting speed: 2.75–3 m/min,
(3) Depth of molten pool: 285–300 mm,
(4) Rolling thickness: 8.5–9 mm.

The lead alloy strips are casted with the use of the optimum parameters. They are shown in Fig. 16.

In order to verify the performance of the TRC lead, the conductivity and mechanical properties are compared between the TRC lead and the traditional process of lead strip. The result of the conductivity is shown in Table 3.

In order to test the mechanical properties, the lead strips which were obtained from two kinds of casting process were sampled in the direction of horizontal, vertical and 45 degrees to the horizontal level. Three samples were taken in each direction. The geometrical size of the tensile specimen is shown in Fig. 17. The tensile experiments are

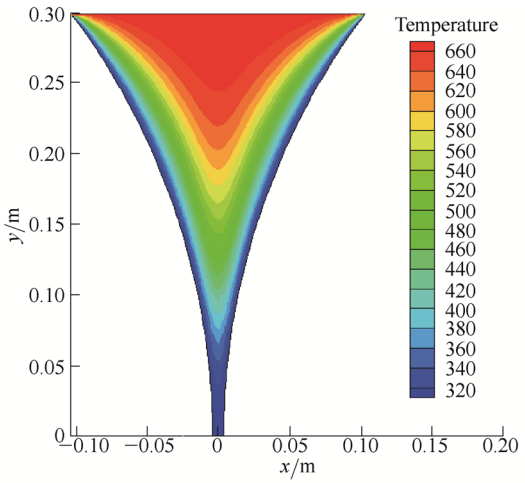

(a) 8 mm

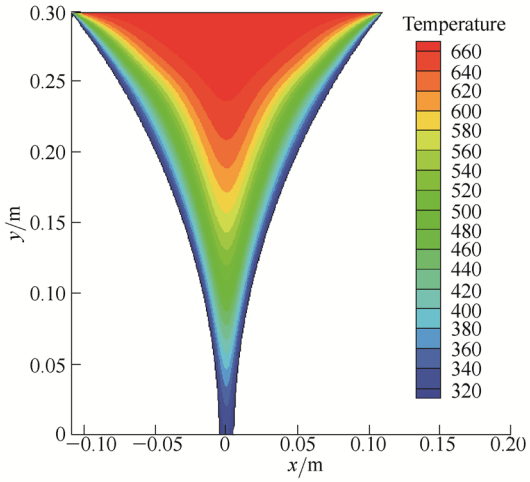

(b) 9 mm

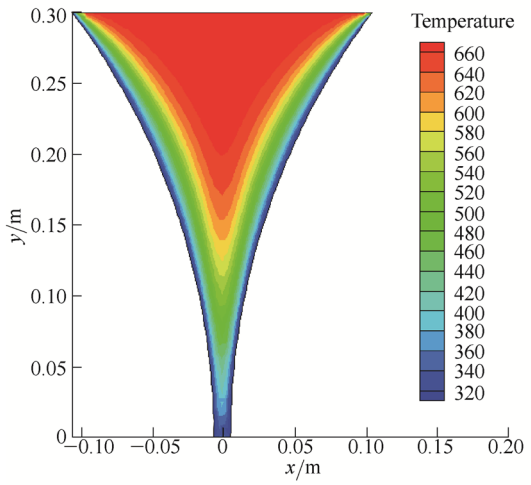

(c) 10 mm

Fig. 13 Temperature contour map of casting under different rolling thicknesses

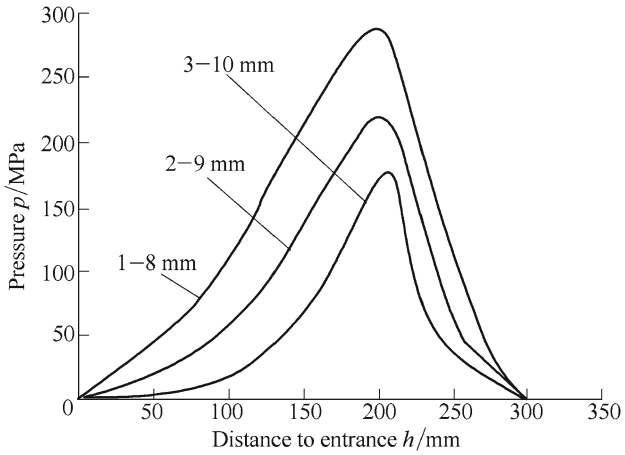

Fig. 14 Influence of rolling thickness on the rolling pressure

(a) Experimental prototype **(b)** Lead molten pool

Fig. 15 Process system of continuous casting of TRC lead

Table 2 Allocation of parameters of sheet of continuous casting process of lead

Factor		*A*	*B*	*C*	*D*
Level	1	360–375	250–265	2.5	8
	2	375–390	265–285	2.75	8.5
	3	390–400	285–300	3	9

A—Pouring temperature *T*/°C, *B*—Depth of molten pool h_m/mm, *C*—Roll casting speed v_R/(m·min^{-1}), *D*—Rolling thickness h_R/mm

Fig. 16 Continuous casting of lead

Table 3 Conductivity of lead strips

Sample	Section size/ (mm × mm)	Length/ cm	Conductivity/ IACS
Traditional process	10 × 3	10	7.98
TRC	9 × 3.1	10	8.23

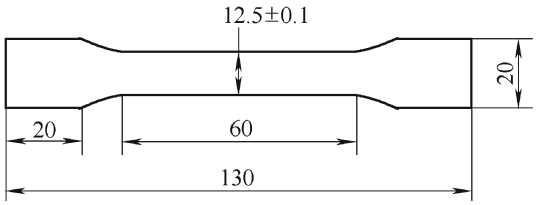

Fig. 17 Geometrical size of the tensile specimen

carried out on the WPL-250 static and dynamic universal testing machine. The mechanical properties of the experimental samples are compared finally.

The hardness test were done on the HW-187.5 Vivtorinox hardness tester, and the data were transferred by using $F/D^2 = 1.25$.

The tensile and hardness test results are shown in Table 4.

From Table 3 and Table 4, the following can be seen:

(1) The conductivity of TRC lead with 8.23 IACS is superior to the traditional process of lead strip with 7.98 IACS.

(2) The traditional casting lead tensile strength of longitudinal is greater than transverse which is 3.31 MPa, its yield strength of longitudinal is greater than transverse which is 1.22 MPa. The TRC lead tensile strength of longitudinal is smaller than transverse which is only 0.53 MPa and yield strength of longitudinal is smaller than transverse which is only 0.81 MPa. From the above data it can be seen that the anisotropic of TRC lead is smaller than the anisotropic of traditional casting lead.

(3) The average tensile strength, the average yield strength and the average elongation of TRC lead is increased by 38.3, 34.1 and 18.2% compared to the traditional casting of lead.

5 Conclusions

(1) The thermodynamic model for TRC lead is built.

(2) Based on the thermodynamic model, the behavior of the TRC process is simulated with the use of Fluent. Through the thermodynamic analysis, the process parameters of cast rolling lead strip can be obtained.

(3) The optimal parameters can be gained with the use of the orthogonal experiment. Finally, the engineering test of TRC lead alloy strip is carried out. The test proves the thermodynamic model is scientific,

Table 4 Mechanical properties of lead strips

Sample	Direction	Tensile strength σ_b/MPa	Yield strength $\sigma_{p0.2}$/MPa	Elongation δ/%	Hardness/HBS
Traditional process	Transverse	25.38	18.32	15	10.5
	longitudinal	28.69	19.54	23	
	45°	29.37	21.31	23	
TRC	Transverse	38.07	26.30	18	12.3
	longitudinal	38.60	26.48	26	
	45°	38.74	26.58	28	

necessary and correct and shows a better conductivity and higher mechanical performance compared to the multi-pass rolling process.

References

1. ZHANG W, HOULACHI G. Electrochemical studies of the performance of different Pb-Ag anodes during and after zinc electrowinning[J]. *Hydrometallurgy*, 2010, 104(2): 129–135.
2. JIANG L X, LV X J, LI Y, et al. Anti-sandwich structure lead-based composite porous anode for zinc electrowinning[J]. *Journal of Central South University*(*Science and Technology*), 2011, 42(04): 871–875. (in Chinese)
3. LUPI C, PILONE D. New lead alloy anodes and organic depolarizer utilization in zinc electrowinning[J]. *Hydrometallurgy*, 1997, 44(3): 347–358.
4. PERKINS J, EDWARDS G R. Microstructural control in lead alloys for storage battery application[J]. *Journal of Materials Science*, 1975, 10(1): 136–158.
5. FELDER A, PRENGAMAN R D. Lead alloys for permanent anodes in the nonferrous metals industry[J]. *Jom the Journal of the Minerals Metals & Materials Society*, 2006, 58(10): 28–31.
6. TARIQ F, AZHER S U, NAZ N. Failure analysis of cast lead-antimony battery grids[J]. *Journal of Failure Analysis & Prevention*, 2010, 10(2): 152–160.
7. PRENGAMAN R D. The metallurgy and performance of cast and rolled lead alloys for battery grids[J]. *Journal of Power Sources*, 1997, 67(1): 267–278.
8. MANDERS J E, LAM L T, PETERS K, et al. Lead/acid battery technology[J]. *Journal of Power Sources*, 1996, 59(1–2): 199–207.
9. PETROVA M, NONCHEVA Z, DOBREV T, et al. Investigation of the processes of obtaining plastic treatment and electrochemical behaviour of lead alloys in their capacity as anodes during the electroextraction of zinc I. Behaviour of Pb-Ag, Pb-Ca and PB-Ag-Ca alloys[J]. *Hydrometallurgy*, 1996, 40(3): 293–318.
10. RASHKOV S, STEFANOV Y, NONCHEVA Z, et al. Investigation of the processes of obtaining plastic treatment and electrochemical behaviour of lead alloys in their capacity as anodes during the electroextraction of zinc II. Electrochemical formation of phase layers on binary Pb-Ag and Pb-Ca, and ternary Pb-Ag-Ca alloys in a sulphuric-acid electrolyte for zinc electroextraction[J]. *Hydrometallurgy*, 1996, 40(3): 319–334.
11. PETROVA M, STEFANOV Y, NONCHEVA Z, et al. Electrochemical behaviour of lead alloys as anodes in zinc electrowinning[J]. *British Corrosion Journal*, 1999, 34(34): 198–200.
12. HILGER J P. How to decrease overaging in Pb-Ca-Sn alloys[J]. *Journal of Power Sources*, 1998, 72(2): 184–188.
13. ALBERT L, CHABROL A, TORCHEUX L, et al. Improved lead alloys for lead/acid positive grids in electric-vehicle applications[J]. *Journal of Power Sources*, 1997, 67(1–2): 257–265.
14. FU K, ZANG Y, GAO Z, et al. Non-linear dynamics of inlet film thickness during unsteady rolling process[J]. *Chinese Journal of Mechanical Engineering*, 2016, 29(3): 1–9.
15. WILSON W R D, LEE W. Mechanics of Surface Roughening in Metal Forming Processes[J]. *Journal of Manufacturing Science & Engineering,* 2001, 123(2):279–283.
16. RASP W, WICHERN C M. Effects of surface-topography directionality and lubrication condition on frictional behavior during plastic deformation[J]. *Journal of Materials Processing Technology*, 2002, 125(2002): 379–386.
17. JESWIET J. A comparison of friction coefficients in cold rolling[J]. *Journal of Materials Processing Technology*, 1998, 80(98): 239–244.
18. TSAO Y H, SARGENT L B. A mixed lubrication model for cold rolling of metals[J]. *ASLE Transactions*, 1977, 20(1): 55–63.
19. YU Y, WANG H, QIANG L I, et al. Finite element simulation of flexible roll forming with supplemented material data and the experimental verification[J]. *Chinese Journal of Mechanical Engineering*, 2015, 29(2): 342–350.
20. WANG X C, YANG Q, HE F, et al. High-precision thickness setting models for titanium alloy plate cold rolling without tension[J]. *Chinese Journal of Mechanical Engineering*, 2015, 28(2): 422–429.
21. LI J P, ZHANG J F, MAO D H, et al. Experimental research on horizontal twin-roller continuous casting lead alloys[J]. *Journal of Huazhong University of Science and Technology*(*Natural Science Edition*), 2010, 38(10): 96–99. (in Chinese)
22. NEH K, ULLMANN M, OSWALD M, et al. Twin roll casting and strip rolling of several magnesium alloys[J]. *Materials Today Proceedings*, 2015, 2(1): 45–52.
23. SUN J Q. *The heat transfer analysis in the process of continuous casting and rolling process*[M]. Beijing: Metallurgical Industry Press, 2010. (in Chinese)
24. WANG X D, XIAO P, YIN S H, et al. Non-uniformity of mould heat transfer and distortion during wide and thick slab continuous casting[J]. *Chinese Journal of Mechanical Engineering*, 2014, 50(22): 28–33. (in Chinese)
25. CUI X C, MA C S, LIU C, et al. Effects on solidification conduct heat and mechanical performance by molten steel vortex flowing in a mould[J]. *Chinese Journal of Mechanical Engineering*, 2003, 39(5): 134–138. (in Chinese)
26. LALLY B, BIEGLER L, HENEIN H. Finite difference heat-transfer modeling for continuous casting[J]. *Metallurgical & Materials Transactions B*, 1990, 21(4): 761–770.
27. TAO W Q. *Numerical heat transfer* [M]. 2nd ed. Xi'an: Xi'an Jiaotong University Press, 2001. (in Chinese)
28. LIAO C R, CHEN R X. The rigid-viscoplastic finit element analysis of non-stationary flow of metals in the edge rolling[J]. *Journal of Chongqing University*, 1990, 13(2): 15–20. (in Chinese)
29. ZHANG D H, LIU Y M, ZHAO D W, et al. Analysis of rolling forces about symmetric and anti-symmetric parabola dog-bone model in vertical rolling[J]. *Journal of Northeastern University*(*Natural Scinece*), 2015, 36(12): 1710–1714. (in Chinese)
30. YING H B. *Analysis of thermo-mechanical behaviors in the mould for small round billet continuous casting*[D]. Dalian: Dalian University of Technology, 2005. (in Chinese)
31. LYON R N. *Liquid metal handbook*[M]. Washington: Government Printing Office, 1952: 21–30.
32. KUTATELADZE S S, BORISHANSKII V M, NOVIKOV I I, et al. *Liquid-metal heat transfer media*[M]. New York: Atomic Press, 1959: 32–35.
33. HULTGREN R, DESAI P D, HAWKINS D T, et al. *Selected values of the thermodynamic properties of binary alloys*[M]. Washington: American Society for Metals, 1973: 41–47.
34. IIDA T, GUTHRIE R I L. *The physical properties of liquid metals*[M]. Oxford: Clarendon, 1988: 78–91.
35. ZHU H J, LIN Y H, XIE L H. *The project cases of fluid analysis of Fluent*[M]. Beijing: Electronic Industry Press, 2011. (in Chinese)

Chengcan JIANG born in 1988, is currently a PhD candidate at *School of Mechanical and Electric Engineering*, *Soochow University*, *China*. He received his master degree on mechatronics from *Soochow University*, *China*, in 2013. His research interests include advanced manufacturing technology, green battery equipment technology and mechatronics product innovation research. Tel: 13506211503; E-mail: jiang198854@163.com.

Yannian RUI born in 1951, is currently a professor at *School of Mechanical and Electric Engineering*, *Soochow University*, *China*. His research interests include mechanical and electrical integration theory, advanced manufacturing technology, environmental protection process equipment and its control and artificial intelligence control. E-mail: ryn1951@sina.com